Supplement of Atmos. Chem. Phys., 16, 11477–11496, 2016
http://www.atmos-chem-phys.net/16/11477/2016/
doi:10.5194/acp-16-11477-2016-supplement

Atmospheric Chemistry and Physics Open Access EGU

Supplement of

A comparative study of K-rich and Na/Ca-rich feldspar ice-nucleating particles in a nanoliter droplet freezing assay

Andreas Peckhaus et al.

Correspondence to: Alexei Kiselev (alexei.kiselev@kit.edu)

S1 Estimation of surface area per droplet

The SEM (FEI QUANTA 650 FEG) was used to measure the surface area of particles in the FS02 suspension droplets. The SEM images taken at different resolution (Fig. S1) were used to estimate the total projection area and the size distribution of the residual particles left after the droplet was evaporated. The projection area of individual residual particles has been measured with the program ImageJ 1.47v and used for derivation of the area equivalent particle diameter assuming particle sphericity. The projection area equivalent diameter of residual particles can either be converted into a size distribution by counting the frequency of residual particle diameters or to a total particle surface area per droplet by summing up the area of individual residual particles. The particle surface area derived from SEM images was in a good agreement with the BET-based particle SSA (see Fig. S2). This led to the assumption that the initial prepared concentrations were close to the final concentrations in the water droplets. Coagulation of feldspar particles in suspension may play a minor rule in concentrated feldspar suspensions (Emersic et al., 2015) but was not observed in this study. Having demonstrated that the $S_{p,\,SEM} = S_{p,\,BET}$ for FS02 at the concentrations used in this work, we have relied on the $S_{p,\,BET}$ measurements for all other feldspar samples.

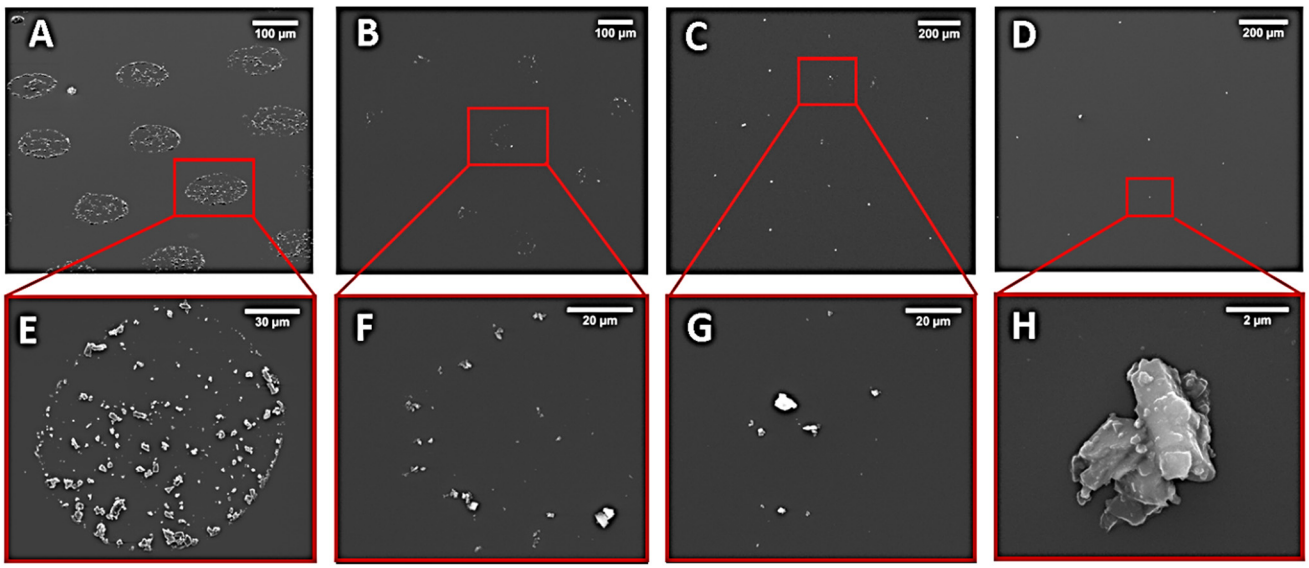

Figure S1: Footprints of the FS02 suspension droplets left after evaporation on the Si-wafer observed in the electron microscope: A) 0.8 wt%, B) 0.1 wt%, C) 0.05 wt% and D) 0.01 wt%. E)-H) Close-up SEM images showing residual particles of individual droplets.

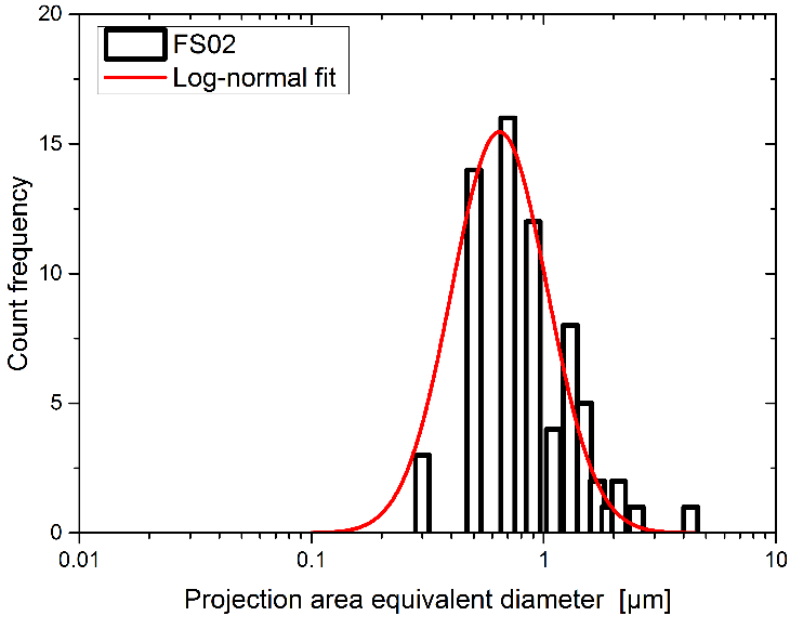

Figure S2: Size distribution of FS02 residual particles (0.1 wt% suspension).

The size distribution of FS02 particles ranged from 0.3µm to 4µm. The maximum is located at approximately 0.7 µm (see **Fig. S2**). The size distribution estimated from SEM images of residual FS02 particles agreed well with the size distribution obtained using laser diffraction analysis (Atkinson et al., 2013). The resolution of SEM images is restricted to serval hundreds of nanometers, which limited the detection of very small FS02 particles.

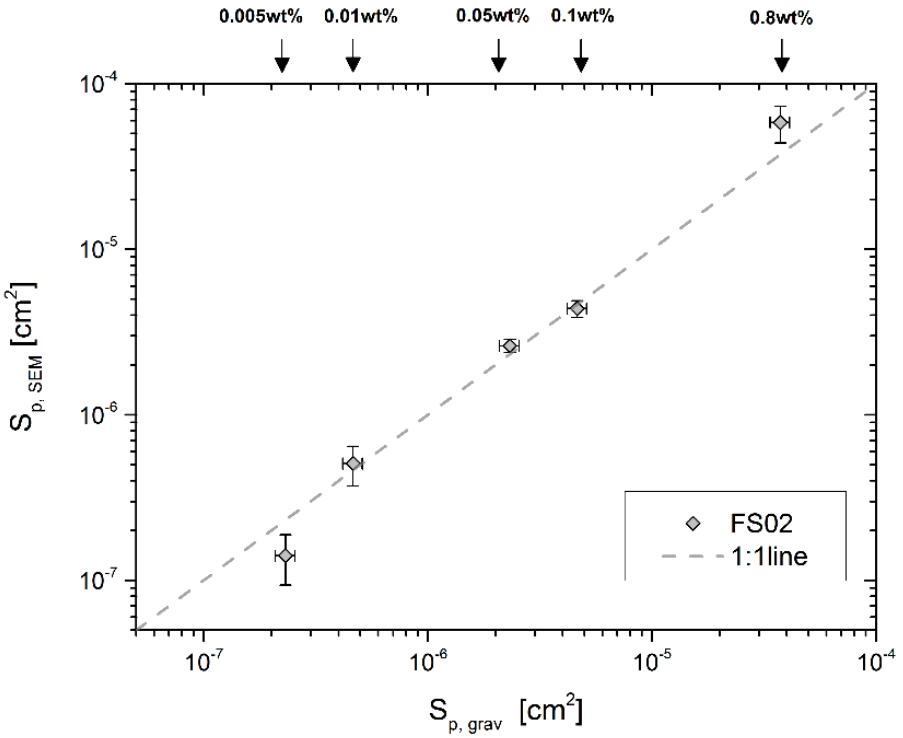

Figure S3: Particle surface area per droplet S_p derived from SEM images ($S_{p,\,SEM}$) versus BET-based particle surface area per droplet ($S_{p,\,grav}$). The black arrows in the top of the panel indicate the corresponding weight percentages.

5

S3 Raman spectra of feldspar samples

Raman spectra of feldspar powder samples were recorded with an inversed optical microscope (Olympus, IX71 with MPlan 20x/50x objective) coupled to a dispersive Raman spectrometer (Bruker, Senterra). For acquisition of bulk spectra, feldspar samples were compressed into a pellets of 5 mm in diameter and excited by a NiYAG laser at wavelength of 532 nm and a
10 power of 50 mW.

The feldspar samples FS02, FS01 and FS04 exhibited Raman bands in the range from 420cm^{-1} to 560cm^{-1} three bands (511cm^{-1}, 474cm^{-1} and 452cm^{-1}), which are characteristic for K-feldspar of microcline variety (Freeman et al., 2008) (see Fig. S4). In the same region, only two bands appeared at 507 cm^{-1} and 479 cm^{-1} for the feldspar sample FS05. The Raman spectra of FS05 could not be clearly associated with albite (Makreski et al., 2009) or andesine (Mernagh, T. P., 1991). No evidence
15 for typical vibration bands of organic compounds was found in the Raman spectra of any of the feldspar samples. Thus, the Raman spectra confirmed mainly the EDX and XRD results with regard to the composition of the feldspar samples.

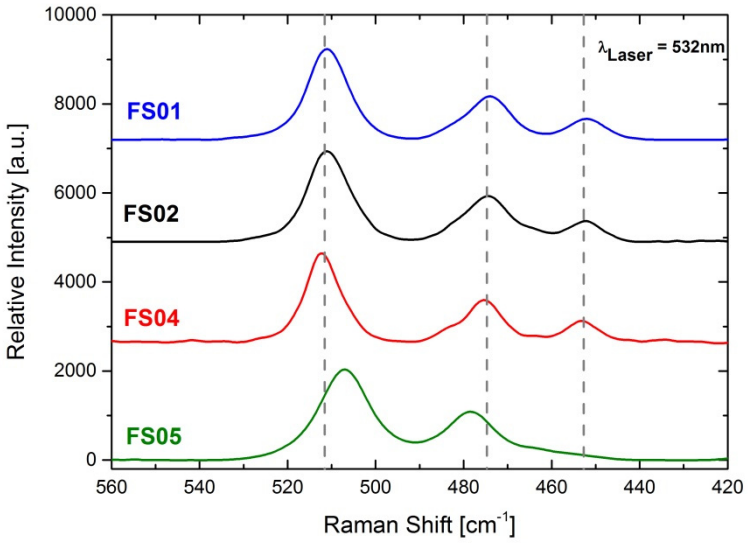

Figure S4: Raman spectra of investigated feldspar particles.

5

S4 Size distribution of FS02 suspension droplets

The volume of the droplets on the Si substrate have been evaluated using equation for the spherical cap geometry (Bourges-Monnier, 1995)

10 $$V = \frac{\pi r^3 (2 - 3cos\alpha + cos^3\alpha)}{3(sin^3\alpha)} \quad \text{(S1)}$$

with r being the apparent radius of the droplet projection on a plane and α the stationary contact angle of water on the substrate. The contact angle was measured optically with the droplets on the substrate cooled down to the dew point temperature of the lab air to avoid the evaporation and was found to be 74° ± 10°. The projection area equivalent diameter (apparent diameter)
15 was measured using the image of the droplet array recorded by the video camera regularly used in the cold stage setup. The distribution of the apparent diameter was found to be centered around (107 ± 14) µm (Fig.S5). Based on these measurements, the average volume of the droplet was evaluated as (215 ± 70) pL.

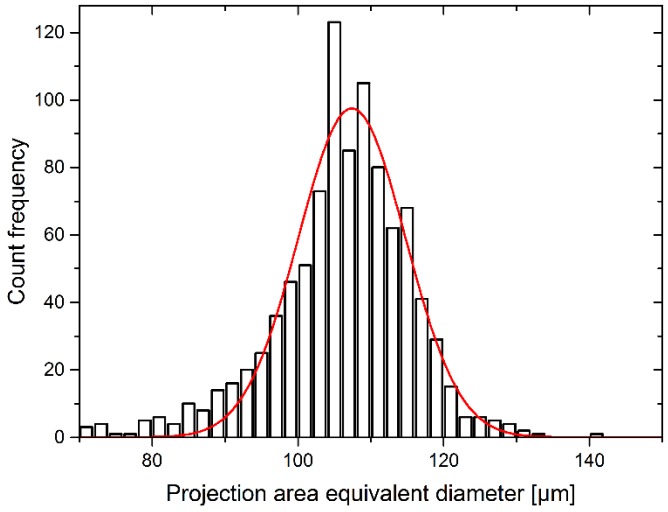

Figure S5: Size distribution of FS02 suspension droplets.

S5 Release of framework cations in aqueous suspensions

The effect of particle processing, such as removal of hydrophilic ions by water, in a water suspension was examined by ion chromatography (IC). Suspended samples were prepared by stirring feldspar suspension (0.1 g in 10 mL of Nanopure water) over one month. IC (Dionex DX-500 IC System equipped with Dionex CD20 Conductivity Detector) was used to determine the concentrations of washed out cations (K^+, Na^+, Ca^{2+} and Mg^{2+}) as a function of time. A weak solution of sulfuric acid (5mL H_2SO_4 (96 wt%) diluted in 2 L of Nanopure water) was used as the eluent. The measurements were conducted every 10 s within first 2 minutes, every 10 min within the first hour after immersion and then every 3 days for a 4-week period. The concentration of K^+ in the washing water of FS01 was steadily rising even after one month in the suspension (Fig. S6), whereas the concentrations of Na^+ and Ca^{2+} in the FS05 suspension were gradually levelling off towards the end of the measurement period.

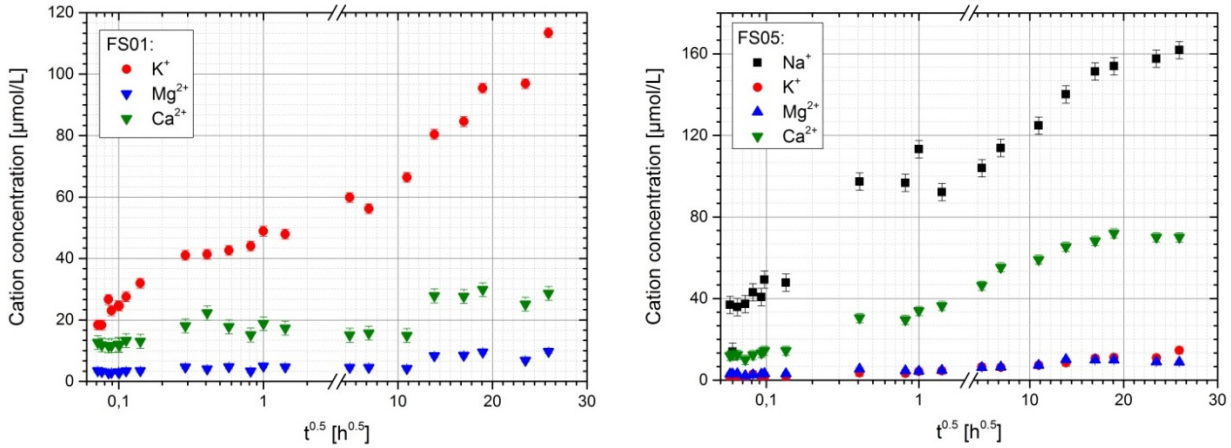

Figure S6: *Evolution of cation concentration in aqueous suspensions of 0.1g feldspar in 10ml deionized water with time derived from ion chromatography (IC) measurements. Left panel: FS01 and right panel: FS05.*

S7 References

Atkinson, J. D., Murray, B. J., Woodhouse, M. T., Whale, T. F., Baustian, K. J., Carslaw, K. S., Dobbie, S., O'Sullivan, D., Malkin, T. L., O'Sullivan, D., The importance of feldspar for ice nucleation by mineral dust in mixed-phase clouds., Nature, 498(7454), 355–8, 2013.

Bourges-Monnier, C., and Shanahan, M. E. R., Influence of Evaporation on Contact Angle, Langmuir 11 (7), 2820-2829, DOI: 10.1021/la00007a076, 1995.

Emersic, C., Connolly, P. J., Boult, S., Campana, M., and Li, Z.: Investigating the discrepancy between wet-suspension- and dry-dispersion-derived ice nucleation efficiency of mineral particles, Atmos. Chem. Phys., 15, 11311-11326, doi:10.5194/acp-15-11311-2015, 2015.

Freeman, J. J., Wang, A., Kuebler, K. E., Jolliff, B. L. and Haskin, L. A.: Characterization of natural feldspars by Raman spectroscopy for future planetary exploration, Can. Mineral., 46(6), 1477–1500, doi:10.3749/canmin.46.6.1477, 2008.

Makreski, P., Jovanovski, G. and Kaitner, B.: Minerals from Macedonia. XXIV. Spectra-structure characterization of tectosilicates, J. Mol. Struct., 924–926, 413–419, doi:http://dx.doi.org/10.1016/j.molstruc.2009.01.001, 2009.

Mernagh, T. P.: Use of the laser Raman microprobe for discrimination amongst feldspar minerals, J. Raman Spectrosc., 22(8), 453–457, doi:10.1002/jrs.1250220806, 1991.